Nanosized Mesoporous Silica Coatings on Ceramic Foams: New Hierarchical Rigid Monoliths

Lenin Huerta,[†,‡] Jamal El Haskouri,[†] David Vie,[†] Maria Comes,[§] Julio Latorre,[†] Carmen Guillem,[†] M. Dolores Marcos,[§] Ramón Martínez-Mañez,[§] Aurelio Beltrán,[†] Daniel Beltrán,[†] and Pedro Amorós*[,†]

Institut de Ciència dels Materials (ICMUV), Universitat de València, P. O. Box 2085, 46071 Valencia, Spain, Departamento de Química, Facultad de Ciencias, Universidad del Zulia, P.O. Box 526, Maracaibo, Venezuela, and Instituto de Química Molecular Aplicada (IQMA), Departamento de Química, Universidad Politécnica de Valencia, Camino de Vera s/n, 46022, Valencia, Spain

Received November 24, 2006. Revised Manuscript Received December 22, 2006

Silica-based rigid monoliths exhibiting a trimodal hierarchical pore system have been successfully prepared through coating of a ceramic foam (CF) with sub-micro-/nanometric mesoporous particles (as building blocks). We have selected a bimodal porous silica, denoted as UVM-7 (a nanometric version of the well-known MCM-41 materials), consisting of small aggregates of nanometric surfactant-assisted mesoporous particles. A colloidal suspension of this material in water is used to coat through successive impregnation cycles the CF surface. The small intraparticle mesopore system (with pore diameters around 2−3 nm) is due to the supramolecular templating effect of the surfactant. Textural large-mesopores/macropores (in the 20−70 nm range) have their origin in the interparticle UVM-7 voids. The large macrocellular macropores are due to the CF support. The resulting monoliths present a good and homogeneous coverage level. Moreover, these composites display better mechanic properties than those of related silica self-supported monoliths.

Introduction

Monolithic porous reactors, widely used in catalytic environmental applications (such as automotive and stationary emissions control), are currently being considered for a variety of novel applications.[1,2] Indeed, structured catalyst packings are more and more being applied in, among others, low pressure drop reactors, membrane reactors, and distillation units. In this context, ceramic foams represent an emerging category of hosts that can be used as structured catalyst supports.[3] Ceramic foams (CF) possess a unique combination of physicochemical (high porosity and chemical stability) and mechanical (low thermal-expansion coefficients and high specific strength) properties.[4,5] In addition, CF can be easily manufactured by impregnation of an organic template foam with inorganic particles or by in situ polymerization followed by calcination.[6] However, thinking on catalytic applications, the relatively low surface areas of CF (usually below 1 m^2/g) constitute a significant drawback.[7] Although wash coating allows enhancing CF surface areas up to ca. 40 m^2/g, these values remain too low for certain applications. This drawback can be partially solved when the catalytic active species are incorporated into the CF in the form of highly dispersed nanosized particles or layered materials.[8] In these cases, the composite surface area enhancement is provided by the small dimensions of the proper active species. This strategy has been extensively used to prepare a variety of composites (containing simple and mixed oxides and metals) with interesting catalytic properties through direct deposition or impregnation.[8] In fact, the support surface area is not a significant parameter in that kind of catalytic composites because it does not modify the active surface area of the catalyst. Very large catalytically active surface areas are only warranted by providing higher surface areas to the supporting material.

Thus, an adequate route for this purpose consists of the deposition of a high-surface porous solid on the CF surface.[9] To date, this strategy has been used for different research groups to generate zeolitic (silicalite-1, ZSM-5, and HZSM-5) coatings on the CF surfaces.[10−16] The resulting CF−zeolite

* To whom correspondence should be addressed. Fax: +34-963543633. E-mail: pedro.amoros@uv.es.
† Universitat de València.
‡ Universidad del Zulia.
§ Universidad Politécnica de Valencia.

(1) Williams, J. L. *Catal. Today* **1999**, *47*, 169.
(2) Heck, R. M.; Gulati, S.; Farrauto, R. J. *Chem. Eng. J.* **2001**, *82*, 149.
(3) Inui, T. *Appl. Catal.* **1985**, *14*, 83.
(4) Colombo, P. *Adv. Eng. Mater.* **1999**, *1*, 203.
(5) Twiggs, M. V.; Richardson, J. T. *Chem. Eng. Res. Des.* **2002**, *80*, 183.
(6) Schwartzwalder, K.; Somers, H.; Somers, A. V. U.S. Patent 3090094, 1963.
(7) Peng, H. X.; Fan, Z.; Evans, J. R. G.; Busfield, J. J. C. *J. Eur. Ceram. Soc.* **2000**, *20*, 807.
(8) See for example Studart, A. R.; Gonzenbach, U. T.; Tervoort, E.; Gaukler, L. J. *J. Am. Ceram. Soc.* **2006**, *89*, 1771 and references therein. Kim, H.; Lee, S.; Han, Y.; Park, J. *J. Mater. Sci.* **2005**, *40*, 5295. Setiabudi, A.; Makkee, M.; Mouljin, J. A. *Top. Catal.* **2004**, *30/31*, 305.
(9) Schüth, F. *Annu. Rev. Mater. Res.* **2005**, *35*, 209.
(10) Seijger, G. B. F.; Oudshoorn, O. L.; van Kooten, W. E. J.; Jansen, J. C.; van Bekkum, H.; van der Bleek, C. M.; Calis, H. P. A. *Microporous Mesoporous Mater.* **2000**, *39*, 195.
(11) Seijger, G. B. F.; Oudshoorn, O. L.; Boekhorst, A.; van Bekkum, H.; van der Bleek, C. M.; Calis, H. P. A. *Chem. Eng. Sci.* **2001**, *56*, 849.
(12) Buciuman, F.-C.; Kraushaar-Czarnetzki, B. *Catal. Today* **2001**, *69*, 337.

10.1021/cm0628101 CCC: $37.00
Published on Web 02/09/2007

composites display significant relative increases of the BET areas. In some cases, these composites have proven to be catalytically efficient materials,[11,15] which should be a consequence of combining an enhanced accessibility to the active groups (across hierarchic pore systems) with the conservation of the high surface area. So these very open networks would favor diffusion of reagents and products while avoiding undesired pore-blocking phenomena.

As mentioned above, all the reported high surface area CF-based composites involve zeolitic coatings, which have been prepared by dip coating, slurry coating, or in situ synthesis on the ceramic support. In practice, these synthetic approaches make use of the feasibility for obtaining zeolites in the form of stable nanoparticles that act as building blocks covering the CF surface. Silica-based mesoporous MCM-41-like molecular sieves (M41S) constitute a very useful alternative in applications where pore sizes larger than those typical of uniform micropores in zeotypes are required. However, it is not known of any CF-M41S composite, that is to say, there is no report to date dealing with the preparation of large CF-based monoliths using preformed silica mesopous nanoparticles as coating blocks. Although this might be related to the difficulty of having large-scale amounts of mesoporous nanoparticles at one's disposal, we succeeded in preparing large trimodal porous monoliths by using polyurethane foams (large-scale templates) coated with preformed silica mesoporous nanoparticles.[17] Unfortunately, the relatively low mechanical stability of these self-supported monoliths limits their applications. In fact, this constitutes a general problem of self-supported multimodal porous silica monoliths regardless of the specific strategy used (sol−gel, spinodal decomposition, etc.).[18,19] Hence, all these monoliths clearly present lower mechanic capabilities when compared to conventional CF.

Here, we present for the first time the preparation and characterization of CF (surfactant-assisted) mesoporous silica composites in the form of rigid large monoliths having trimodal pore systems (small meso-, large meso-, and macroporous). The monoliths have been synthesized by using preformed mesoporous nanoparticles and a CF as support. The surfactant-assisted synthesis of the silica-based nanoparticulate mesoporous reagent materials has been reported elsewhere.[20] These materials, denoted UVM-7 (a nanometric version of the MCM-41 silicas), show very open architectures consisting of micrometric aggregates of mesoporous nanoparticles connected through covalent bonds. This organization defines two pore systems: the first one (intraparticles) is generated by the effect of the surfactant micelles and the second one (inter-particles) is formed as the nucleation and growth of the primary mesoporous nanoparticles proceeds. Moreover, the micrometric aggregates of the as-synthesized UVM-7 solids can be transformed into even smaller submicrometric or nanometric aggregates by means of high-power ultrasound treatment, which leads to stable colloids in water.[17] This is a key point in our preparative procedure because it allows us to have UVM-7 stable colloidal particles able to cover the CF support by dip coating.

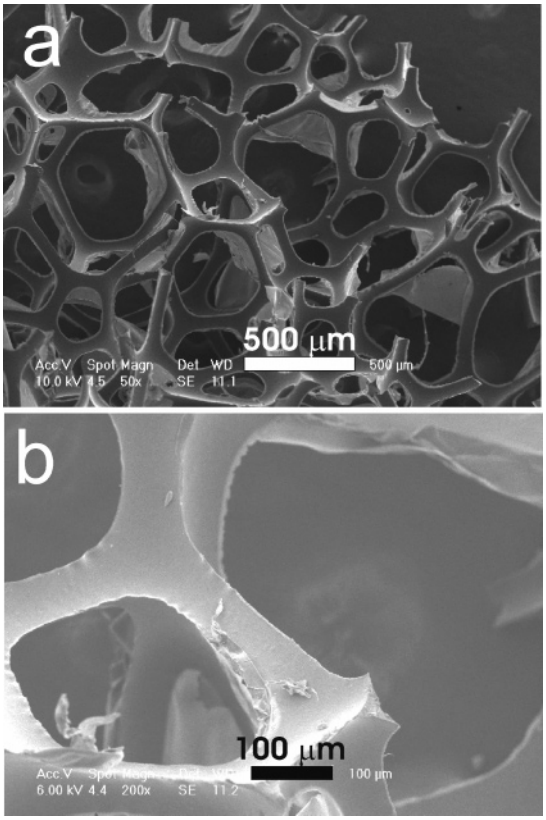

Figure 1. (a) Low- and (b) high-magnification SEM images of the commercial PUF used.

Experimental Section

A simple four-step protocol of a typical synthesis is as follows: (1) preparation and activation of the CF; (2) preparation of the mesoporous/mesostructured material; (3) particle-size reduction (from micro- to submicro- or nanoparticles) by ultrasound irradiation, and (4) coating of the CF.

Step 1. The synthesis of the ceramic foam (CF) was carried out through a typical organic foam replication, a technique that allows good control of the monolith shape and dimensions.[21] Commercially available and inexpensive polyurethane foam (PUF) without cell-forming membranes (average pore diameters around 600 μm (30 ppi)) was used as macroscale template (Figure 1).

The foam was impregnated with an optimally deflocculated casting slip for porcelain bodies prepared with two different kaolins, feldspar and quartz, which contained 67% of solid materials (19.4% kaolin A, 18.1% kaolin B, 10.7% quartz, 18.8% feldspar), and 33% of water, which included the deflocculant (0.45% with respect to solid kaolins), to give a slip density of 1.6 g/cm^3. As deflocculant,

(13) Sterte, J.; Hedlund, J.; Creaser, D.; Öhrman, O.; Zheng, W.; Lassinantti, M.; Li, Q.; Jareman, F. *Catal. Today* **2001**, *69*, 323.
(14) Zampieri, A.; Colombo, P.; Mabande, G. T. P.; Selvam, T.; Schwieger, W.; Scheffler, F. *Adv. Mater.* **2004**, *16*, 819.
(15) Patcas, F. C. *J. Catal.* **2005**, *231*, 194.
(16) Scheffler, F.; Zampieri, A.; Schwieger, W.; Zeschky, J.; Scheffler, M.; Greil, P. *Adv. Appl. Ceram.* **2005**, *104*, 43.
(17) Huerta, L.; Guillem, C.; Latorre, J.; Beltrán, A.; Beltrán, D.; Amorós, P. *Chem. Commun.* **2003**, 1448.
(18) Brandhuber, D.; Peterlik, H.; Hüsing, N. *J. Mater. Chem.* **2005**, *15*, 3896.
(19) Amatani, T.; Nakanishi, K.; Hirao, K.; Kodaira, T. *Chem. Mater.* **2005**, *17*, 2114.
(20) El Haskouri, J.; Ortiz de Zárate, D.; Guillem, C.; Latorre, J.; Caldés, M.; Beltrán, A.; Beltrán, D.; Descalzo, A. B.; Rodríguez, G.; Martínez, R.; Marcos, M. D.; Amorós, P. *Chem. Commun.* **2002**, 330.
(21) Schwartzwalder, K.; Somers, A. V. Method of Making a Porous Shape of Sintered Refractory Ceramic Articles. U.S. Patent 3090094, 1963.

a mixture of sodium carbonate ($Na_2CO_3 \cdot 10H_2O$) and sodium silicate (aqueous solution with a density of 1.36) in a weight ratio of 2:1 was used. The green body obtained with this slip had the following chemical composition: SiO_2, 68.0%; Al_2O_3, 21.5%; Na_2O, 0.8%; K_2O, 4.1%; ignition loss, 5.6%; distributed as kaolinite, quartz, and feldspar minerals. The corresponding porcelain body (after firing at 1300 °C) consisted of a vitreous phase, which contains sodium and potassium aluminosilicates and part of the silica, and two crystalline phases, mullite and quartz.

The impregnated PUF was passed through rollers preset at 80% compression to expel the excessive slurry and dried at room temperature to obtain a coated PUF. Then, the monolith was calcined in a two-step process (at 500 °C for 2 h, and later at 1200° for 5 h) to provoke PUF evolution and ceramic vitrification.

To slightly increase both the CF surface area and a certain surface activation (by inducing the formation of silanol groups), the monolith was placed into an alkaline solution (1 M NaOH) and heated at 110 °C for 2 h. The aim of this activation step was to favor the CF surface coating by facilitating the formation of links (covalent Si−O−Si bonds) with UVM-7 nanoparticles.

Step 2. The nanosized mesoporous UVM-7 silica was synthesized through a one-pot surfactant-assisted procedure in a homogeneous hydroalcoholic reaction medium (water/triethanolamine). The procedure, a modification of the so-called "atrane route",[22] has been recently described in detail.[23] It is based on the use of a simple structural directing agent (CTMABr = cetyltrimethylammonium bromide) and a complexing polyalcohol (triethanolamine), which originates silatrane complexes (relatively inert complexes that include triethanolamine-related ligand species) as hydrolytic precursors. Together with its complexing ability, the presence of the cosolvent (triethanolamine) was a key in order to favor the formation of nanoparticulated materials.[23] To open the intranoparticle mesopores, the surfactant was extracted from the as-synthesized mesostructured solid by chemical exchange using a HCl/ethanol solution ($CTMA^+/H^+$ exchange). In comparison with calcination, chemical extraction favors lesser condensation of the nanoparticles, this leading to smaller aggregates. Indeed, ca. 1 g of mesostructured UVM-7 powder was suspended in a solution containing 16 mL of HCl (37%) and 130 mL of ethanol (99%), and this mixture was heated at reflux (60 °C) for 2 h while stirring. Later, after renewal of the HCl/ethanol solution, and to complete the extraction process, the suspension was heated again at 60 °C for 16 h while stirring. The resulting (mesoporous) powder was collected by filtration, washed with ethanol, and air-dried at 100 °C.

Step 3. The UVM-7 colloidal suspension was prepared by means of ultrasound irradiation in water (using a high-power Branson instrument). In a typical preparation, a suspension containing 2 g of UVM-7 in 100 mL of distilled water (2% in weight) was irradiated for 15 min at a nominal power of 350 W. After irradiation, the suspension has colloidal character showing the Tyndall effect.

Step 4. Finally, the CF coating was performed by successive impregnation cycles in an aqueous UVM-7 colloidal suspension (ca. 2% in weight) followed by soft thermal treatment (120 °C for 2 h) to favor water evolution and nanoparticle condensation (formation of covalent Si−O−Si bonds both among nanoparticles and with the CF surface).

Alternatively, colloidal suspensions of as-synthesized mesostructured UVM-7 silica (with intraparticle mesopores filled with surfactant molecules) can be used to coat the CF. In this case, we have used basically the same experimental protocol with an obvious difference: the chemical exchange to open the mesopore system is suppressed and the CTA^+ molecules are removed through a final calcination step (550 °C for 2 h) of the whole CF−UVM-7 composite. This preparative route leads to similar porous hierarchic monoliths.

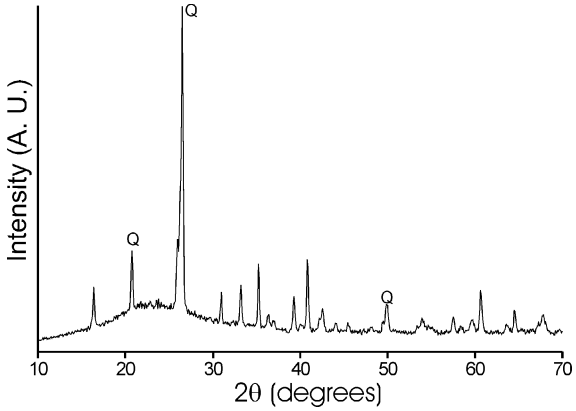

Figure 2. XRD pattern of the CF. Q = quartz. The remaining peaks correspond to mullite.

To appreciate the coating homogeneity along the CF monolith, we used a V-containing derivative, denoted as V−UVM-7, that presented a characteristic yellow color under ambient conditions. This color is due to an intense absorption band in the 370−390 nm range that is assigned to a charge-transfer transition of V(V) species in penta- or hexacoordinated environment originating through hydration of V(V) sites close to the pore surface and, hence, highly accessible to water molecules. We have synthesized a sample with a Si/V= 25 molar ratio following the method described in ref 24.

Characterization Techniques. X-ray powder diffraction (XRD) data were recorded on a Seifert 3000TT $\theta-\theta$ diffractometer using Cu Kα radiation. Both low- and high-angle XRD patterns were recorded to analyze the diffraction signals typical of the UVM-7 mesoporous silicas and the peaks associated with the CF. Low-angle XRD patterns were collected in steps of 0.02°(2θ) over the angular range 0.65−10°(2θ) for 25 s/step. High-angle patterns were collected with a larger scanning step [0.05°(2θ)] over the angular range of 10−70°(2θ) and a lower acquisition time (10 s/step). High- and low-magnification SEM images were recorded by using an Hitachi S-4100 FE or a Philips XL30ESEM microscope, respectively. Samples were previously coated with Au−Pd. A TEM study was carried out with a JEOL JEM-1010 instrument operating at 100 K and equipped with a CCD camera. Samples were gently ground in dodecane, and microparticles were deposited on a holey carbon film supported on a Cu grid. Nitrogen adsorption−desorption isotherms (−196 °C) were recorded with a Micromeritics ASAP-2010 automated instrument. Calcined samples were degassed at 120 °C and 10^{-6} Torr for 5 h prior to measurement. Surface areas were estimated according to the BET model, and pore size dimensions and pore volumes were calculated by using the BJH method from the adsorption branch of the isotherms. Mercury porosimetry curves were recorded with Micromeritics Autopore III equipment. Mechanic properties were evaluated through compression tests using an Instron 5582 instrument. Particle size measurements in the colloidal suspensions were determined through dynamic light scattering by using Malvern Zetasizer Nano-ZS equipment working at 25 °C and using accumulation times of 120 s. These DLS measurements were performed exactly under the same experimental conditions used in Step 4 of our preparative proto-

(22) Cabrera, S.; El Haskouri, J.; Guillem, C.; Latorre, J.; Beltrán, A.; Beltrán, D.; Marcos, M. D.; Amorós, P. *Solid State Sci.* **2000**, *2*, 405.
(23) Huerta, L.; Guillem, C.; Latorre, J.; Beltrán, A.; Martínez-Máñez, R.; Marcos, M. D.; Beltrán, D.; Amorós, P. *Solid State Sci.* **2006**, *8*, 940.
(24) Huerta, L.; Amorós, P.; Beltrán, D.; Cortés-Corberán, V. *Catal. Today* **2006**, *117*, 180.

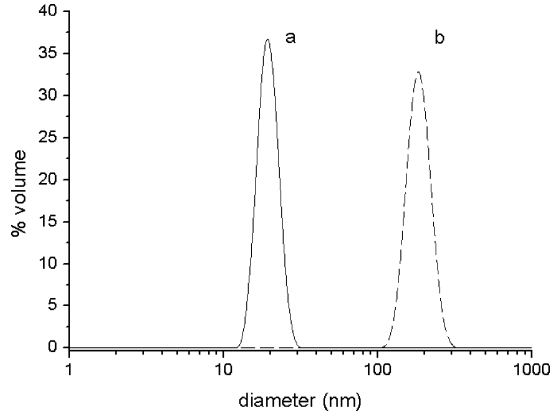

Figure 3. Particle size distribution of UVM-7 colloidal suspensions used to coat the CF. (a) After ultrasound irradiation. (b) After several hours.

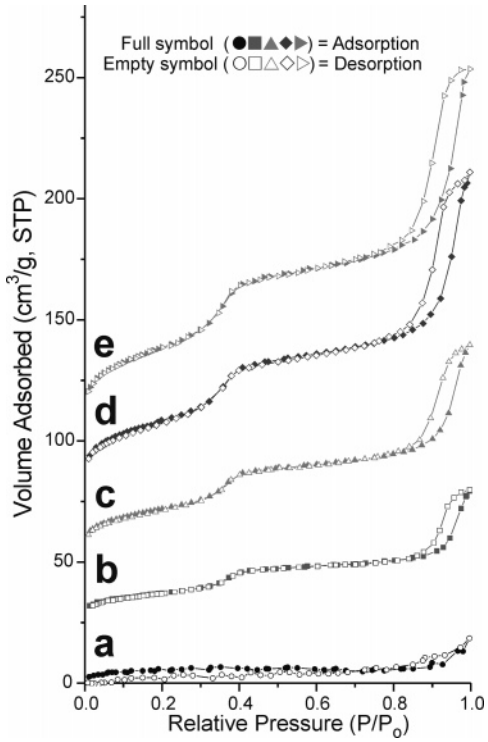

Figure 4. N_2 absorption−desorption isotherms before coating (a), and after one (b), two (c), three (d), and four (e) impregnation cycles. The isotherms are *y*-shifted for clarity.

col: UVM-7 silica concentration of 2% (in weight) and without using specific (deflocculant) organic additives usually added to favor the colloid stabilization. Only under these conditions can we extract conclusions on the process implied in the preparative protocol used. Moreover, we have recorded sequential DLS measurements at different times to analyze the colloid stabilization and dynamic.

Results and Discussion

In contrast to previous works describing zeolitic coatings on CF supports, where alumina or SiC supports were used, we opted for using a slurry of composition 3:1 SiO_2:Al_2O_3 with the aim of obtaining a silica-rich CF. In this way, we looked for enhancing the affinity between the mesoporous UVM-7 particles and the CF surface, which must facilitate the coating processes. The final CF was prepared (step 1) through conventional polyurethane foam (PUF) replica technique (Schwartzwalder process),[21] which allows good control of the monolith shape and dimensions. As expected

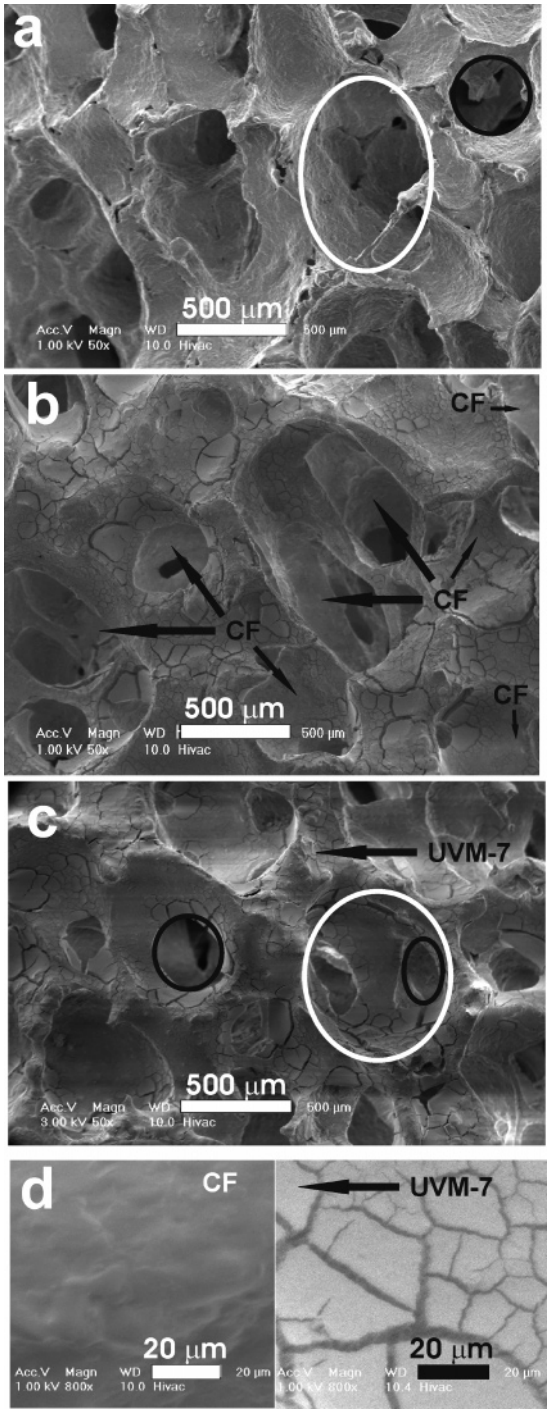

Figure 5. SEM images of the CF before coating (a) and after three (b) and four impregnation cycles (c). Some open cells and their windows are marked in white and black circles, respectively. The image (d) shows a view of the evolution of the surface morphology.

from the $SiO_2-Al_2O_3$ phase diagram, the XRD data (Figure 2) show that the final material is biphasic and basically formed by two crystalline phases: quartz (60%) and mullite (23%) (composition estimated from XRD phase analysis). These crystalline phases coexist with a vitreous phase including amorphous sodium and potassium aluminosilicates. The result is a rigid foamlike macroporous monolith (CF) (wt % composition, after calcination: SiO_2 72.0%, Al_2O_3 22.8%, Na_2O 0.9%, K_2O 4.3%).

Before coating, the CF was washed with alkaline aqueous solutions to both increase the surface area (from 0.47 to 0.95

Table 1. Evolution of the Textural Properties and Coverage Level as the Impregnation Cycles Increase When Colloidal Suspensions of Mesoporous UVM-7 Are Used

coating cycles	BET (m^2/g)	BJH intraparticle pore (nm)	BJH interparticle pore (nm)	small pore volume (cm^3/g)	large pore volume (cm^3/g)	coverage	
						wt %	g/g CF
UVM-7	1110	3.15	45.9	1.13	1.88		
CF	0.95					0	0
1	44	3.12	51.3	0.03	0.05	3.7	0.039
2	80	3.12	48.6	0.06	0.08	6.4	0.067
3	120	3.14	47.1	0.08	0.11	10.3	0.108
4	140	3.13	46.0	0.10	0.13	12.0	0.126

m^2/g) and also to provide a certain surface activation by favoring the increasing of the number of silanol groups. This last treatment does not modify the XRD pattern, and hence, we can assume that both composition and microstructure are maintained. The mercury intrusion porosimetry allows estimating an average macropore of ca. 475 μm, in good accordance with the microscopic images.

To favor an effective and efficient invasion and coating of the CF surface, the average size of the UVM-7 colloidal particles must be significantly lower than the CF macropore and pore-window dimensions. We have studied the particle size distributions in colloidal suspensions through DLS measurements and the results are shown in Figure 3. Immediately after ultrasound irradiation a single and narrow particle size distribution centered at ca. 20 nm is observed. This value fits very well with the average particle dimension observed in TEM images (ca. 20−25 nm). In our preparative protocol, the CF coating is carried out only a few minutes (ca. 3−5 min) after irradiation. Then, we conclude that under these conditions the CF coating is performed by deposition essentially of isolated UVM-7 nanoparticles. Although no precipitation is observed during several hours, the colloid presents a dynamic aggregation evolution from isolated particles to clustered aggregates due to the high reactivity (in water solution without stabilizing agents) of silica nanoparticles with a high density of silanol groups at the particle surface and the natural tendency to the interparticle condensation (formation of Si−O−Si interparticle covalent bonds). In any case, the maximum aggregation observed corresponds to clusters of ca. 180 nm in diameter. This value that corresponds to a maximum limit of particle growth is significantly lower than the CF macropores. Then, we consider that these last aggregates still are adequate and effective at forming a continuous and homogeneous coating on the CF surface. In fact, we have verified that the size of the UVM-7 clusters (from 20 to 180 nm) does not affect the final properties of the final composites when CF with large macropores was used as support. Similar BET surface areas and BJH pore volumes were achieved for similar amounts of UVM-7 material on the CF surface. In our case, the large macropores of the CF allow an easy and efficient diffusion even of the largest detected clusters (of ca. 180 nm). The UVM-7 ultrasound irradiation and the CF coating are performed exactly in the same aqueous media. Then, the same interparticle condensation processes are effective before and after CF coating and consequently similar aggregates are formed.

As shown in Figure 4, the N_2 isotherms of all the resulting composites show the characteristic features of UVM-7 materials: two well-defined adsorption steps at intermediate ($0.3 < P/P_0 < 0.5$) and high ($P/P_0 > 0.8$) relative pressure values, which can be respectively associated with the filling of the intra-nanoparticle (surfactant generated) small mesopores and the interparticle (generated by condensation of the primary nanoparticles) large mesopores. The physisorption data in Table 1 evidence that both the BET surface area and pore volumes in the composite monoliths increase regularly with the number of impregnation cycles. Moreover, the N_2 adsorption ratio associated with the intra- and interparticle pores is practically constant and very similar to that expected for a UVM-7 sample. After four cycles, the relative weight increase of the CF support was 12%, which corresponds to the incorporation of 0.126 g of the mesoporous nanoparticles. Assuming that the 140 m^2/g are basically due to the UVM-7 solid, we can estimate an average BET area of 1111 m^2/g for the pure UVM-7 sample. This value fits very well with typical BET area of UVM-7 derivatives. Then, the high accessibility of the UVM-7 pore systems is preserved even for nanoparticles close to the CF surface. Mercury porosimetry data shows that the open macropore is maintained (pore size of 452 μm).

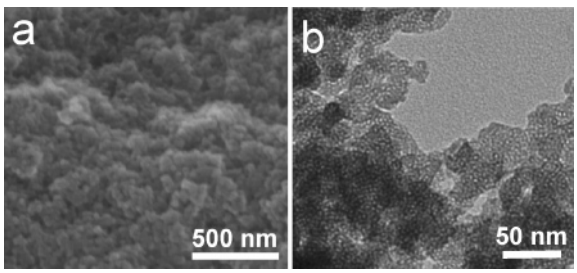

Figure 6. FE-SEM and TEM images showing typical UVM-7 like aggregates (a) and mesoporous nanoparticles (b) in the sample obtained after four impregnation cycles.

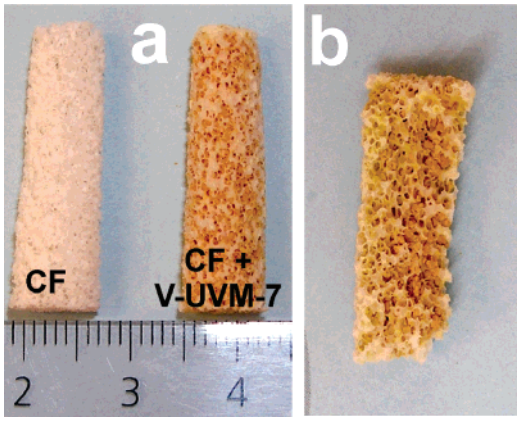

Figure 7. (a) Optical images of CF monoliths before and after coating with a V−UVM-7 colloid showing the homogeneity of the recovery. (b) Image of the interior of the (broken) coated monolith.

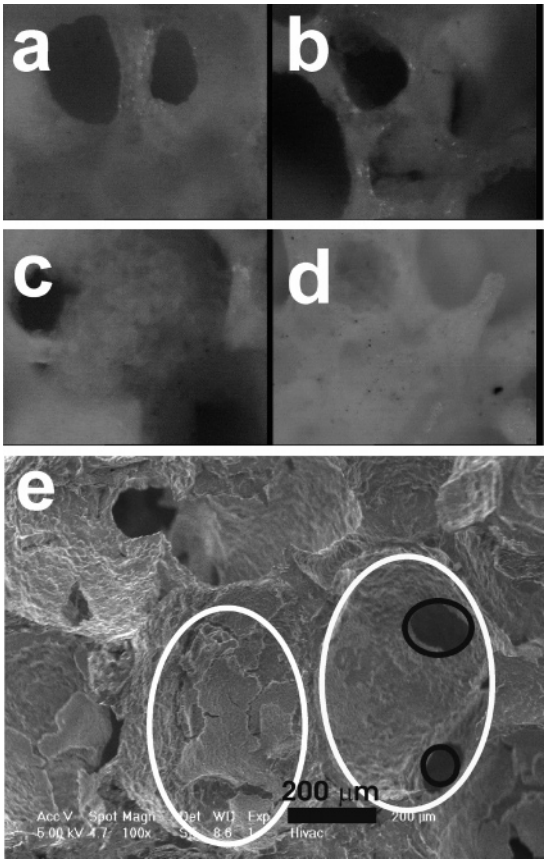

Figure 8. Optical microscopy images of the coated CF after (a) one, (b) four, (c) five, and (d) seven impregnation cycles. (e) SEM image of the CF after seven impregnation cycles. Open macropore windows indicated in black. Partially open and closed foamlike cells are indicated in white.

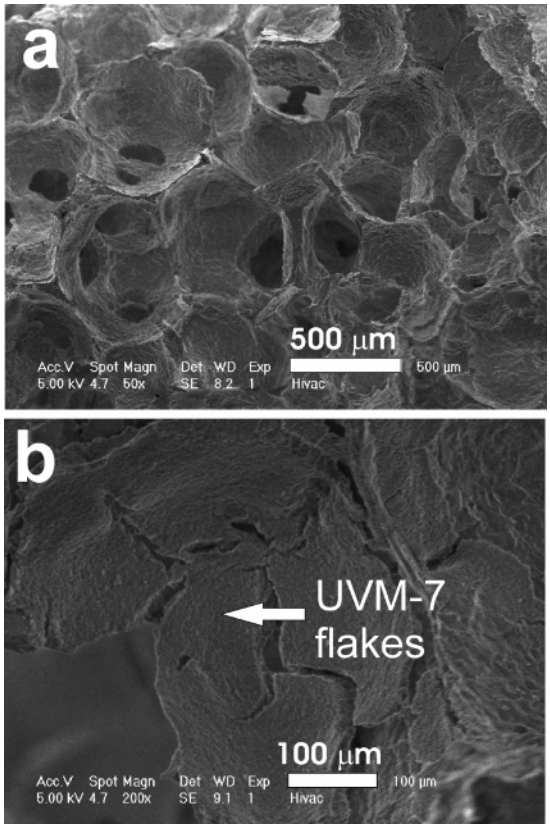

Figure 9. SEM images of the CF after four impregnation cycles with the as-synthesized UVM-7 nanoparticles.

SEM images in Figure 5 show that the ceramic texture is no longer observed after four impregnation cycles, which should be consistent with a complete covering of the CF support. In fact, while small ceramic domains remain uncovered even after three impregnations, after four coating cycles only deposits with UVM-7 texture are observed. The foam coating is rather homogeneous and can be described as formed by successive deposition of small UVM-7 flakes in an imbricate way. These flakes are rather regular and have about 6−9 μm of thickness. The origin of these thick flakes is probably the cracks generated during the drying process. Probably, the macrostructure generated by superposition of the UVM-7 flakes induces a "binder" effect favoring the cohesion of the particles among them. High-magnification SEM and TEM images (Figure 6) demonstrate that the UVM-7 organization is preserved. Thus, at micrometric scale, the deposited silica flakes present rough surfaces (Figure 6a) consisting of aggregates of pseudospherical clusters of mesoporous nanoparticles (Figure 6b), which define true textural large mesopores among them. The intraparticle disordered small mesopore system can be clearly appreciated in Figure 6b. This fact confirms that the intraparticle mesopore organization is preserved after the CF coating. These mesopore systems (small and large) typical of UVM-7, together with the foamlike interconnected macropores (400−600 μm) (Figure 5b), define a very open hierarchical porous architecture.

The preparative technique allows high control of the shape of the final monoliths (Figure 7a), and only a slight shrinkage of ca. 5% with respect to the starting PUF is observed. On the other hand, to appreciate the coating efficiency, we have impregnated four times a CF monolith in a colloidal suspension of V−UVM-7. To characterize optically the CF microstructure, yellow-colored V-containing UVM-7 colloid has been used as impregnating material. The images in Figure 7 show the surface (a) and the interior (longitudinal section) (b) of a CF-coated monolith prepared in that way. These images show the existence of a homogeneous V−UVM-7 coating on the white CF support at macroscopic/micrometric level with a regular and homogeneous yellow color both on the surface and in the interior of the monolith. In practice, there are no appreciable differences in the coating degree between the monolith surface and its interior.

The method also allows modulating the UVM-7 load (see Table 1). After four impregnation cycles, the relative amount of UVM-7 incorporated into the composite rises to 12 wt %. This load value is very similar to those achieved for zeolitic coatings on CF of similar pore sizes and windows. Assuming a complete and uniform covering of the CF surface, and taking into account the typical average density of UVM-7 (ca. 0.4 g/cm^3), it is possible to estimate an average thickness of the coating layer of ca. 31 μm after four impregnations. This value, according to SEM observations, might be associated with the superposition of four UVM-7 flakes of about 7−8 μm. Although further impregnation cycles result in increases of the UVM-7 loads, we have observed that it simultaneously causes blocking of a certain amount of small macropore windows (after five cycles). In fact, after seven impregnations, we have achieved coverage values as high as 17% (0.207 g/g CF; BET = 229

m^2/g), but optical microscopy and SEM images of the resulting monolith show a significant proportion of closed pore windows (with dimensions in the starting CF in the 100−200 μm range). Hence, a significant and progressive blocking of the macropore foamlike windows is clearly appreciated for samples after five and seven dip-coating cycles even from optical microscopy images (Figures 8c and 8d). SEM micrograph of a sample after seven impregnation cycles clearly shows a significant decrease in the number of open macropore windows (Figure 8e).

This same procedure can be applied by using colloidal suspensions of UVM-7 mesostructured (as-synthesized; prior to surfactant removal) nanoparticles. A similar progressive covering of the CF surface is observed (Figure 9). In this case, the surfactant evolution can be made by calcination after formation of the CF−UVM-7 composite. Thus, selection of the specific preparative protocol depends on the final application of the monolith.

In any case, regardless of the preparative strategy (i.e., starting from mesoporous or mesostructured nanoparticles), the final trimodal porous monoliths present good mechanic properties associated with the CF support ($\sigma_t = 3-4$ MPa estimated from a diametrical compression test). These mechanic properties are significantly better than those presented by self-supported monoliths. Similar mechanic properties have been recently reported for silica monoliths prepared through partial fusion of mesoporous silica spheres.[25]

Concluding Remarks

In conclusion, we present here for the first time a simple reproducible strategy to prepare nanosized mesoporous silica coatings on ceramic foams. The final composites show hierarchic trimodal porosity together with good mechanic properties. The very open framework of the resulting monoliths and the versatility to modify both composition and macro- or mesopore size confers on them special interest in areas such as chemical sensors, catalysis, and environmental chemistry.

Acknowledgment. We thank the MCyT (MAT2003-08568-C03 and CTQ2006-15456-C04-03/BQU) and the Generalitat Valenciana (IIARC0/2004/A-175 and A-363) for support. J.E.H. thanks the MEC for a Ramón & Cajal contract. L.H. thanks the Universidad del Zulia for a doctoral grant. M.C. thanks the CAM for a doctoral fellowship.

CM0628101

(25) Vasiliev, P. O.; Shen, Z.; Hodgkins, R. P.; Bergström, L. *Chem. Mater.* **2006**, *18*, 4933.